

## **Electronic Supplementary Information**

### **Two-dimensional iron MOF nanosheet as a highly efficient nanozyme for glucose biosensing**

Ai Yuan, Yuwan Lu, Xiaodan Zhang, Qiumeng Chen, Yuming Huang\*

College of Chemistry and Chemical Engineering, Southwest University, Chongqing  
400715, China

*\*Corresponding author. E-mail: [ymhuang@swu.edu.cn](mailto:ymhuang@swu.edu.cn)*

## Reagents and instrumentation

All chemical reagents were of analytical grade and used as received. Glucose, fructose, lactose, and maltose were purchased from Sinopharm Chemical Reagent (Shanghai, China). Glucose oxidase (GODx, EC1.1.3.4.47, 200 U/mg) and 3,3',5,5'-tetramethylbenzidine (TMB) were purchased from Sigma-Aldrich (Shanghai, China). H<sub>2</sub>O<sub>2</sub>, ferric nitrate nonahydrate (Fe(NO<sub>3</sub>)<sub>3</sub>·9H<sub>2</sub>O), ferric chloride hexahydrate (FeCl<sub>3</sub>·6H<sub>2</sub>O), acetic acid, sodium acetate, polyvinylpyrrolidone (PVP), 1,3,5-benzenetricarboxylic acid (H<sub>3</sub>BTC), copper chloride dihydrate (CuCl<sub>2</sub>·2H<sub>2</sub>O), ascorbic acid (AA) and ethanol were obtained from Chongqing Taixin Chemical Reagents Company (Chongqing, China). Serum samples were obtained from local hospital. Ultra-filtration tubes with cutoff molecular weight of 30 kDa were provided by Millipore Corporation (Billerica, MA 01821, USA).

UV-vis spectra were recorded on a UV-2450 spectrophotometer (Suzhou, Shimadzu). The scanning electron microscope (SEM) image was taken on a Hitachi model S-4800 field emission scanning electron microscope (Hitachi, Japan). The X-ray diffraction (XRD) data were acquired on a XD-3 X-ray diffractometer (PuXi, Beijing). X-ray photoelectron spectroscopy (XPS) characterization was conducted by using a VG Multilab 2000X instrument (Thermal Electron, USA). Fourier transform infrared (FT-IR) spectra were obtained using a Tenson 27 Fourier Transform Infrared spectrometer (Bruker, Germany). Atomic force microscopy (AFM) characterization was carried out on a SPA400 instrument (Seiko, Japan).

## Calculation of the $K_w$ value

To assess the catalytic activity of 2D Fe-BTC nanozyme, we used the  $K_w$  value, which is defined as the TMB oxidation rate or H<sub>2</sub>O<sub>2</sub> reduction rate catalyzed by unit mass concentration of catalyst. It is a measure of the rate at which a catalyst catalyzes a reaction, and can be calculated by the equation (1):

$$K_w = V_{\max}/w \quad (1)$$

where  $V_{\max}$  is the maximal reaction velocity, and  $w$  is the mass concentration of catalyst. The calculated  $K_w$  values for different nanozymes are summarized in Table 1.

### **Fe leaching under pH 3.5 acidic condition**

To examine the released Fe content, the 2D Fe-BTC was immersed in 0.2 M acetate buffer (pH 3.5) for 15 min. Then the leachate was obtained by 0.22  $\mu\text{m}$  membrane filtration and used for Fe determination using flame atomic absorption spectrometry. Also, the total Fe content in catalyst was determined after the acid digestion of 2D Fe-BTC. The Fe content in leachate was 0.0097 mg/g, and the total Fe content in 2D Fe-BTC solid was 0.212 mg/g. Thus, only 4.6% Fe was released under pH 3.5 condition. So, the enzyme-like activity was ascribed to the 2D Fe-BTC MOF itself.

### **XPS spectra of physically mixed Fe added to Cu(HBTC)**

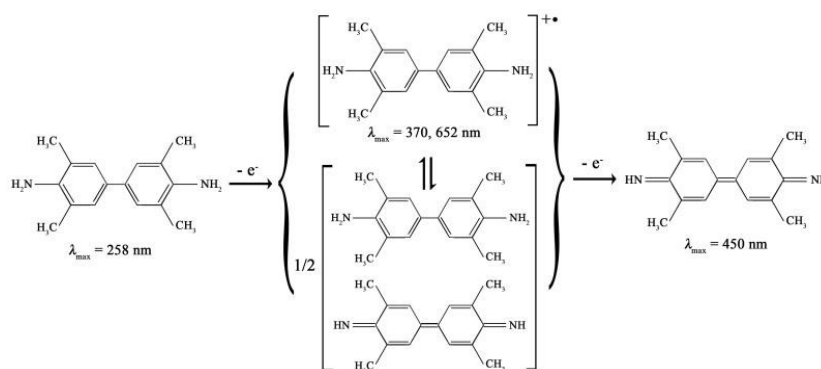
The physically mixed 10 mg of Cu(HBTC)-1 and 30 mg of  $\text{FeCl}_3$  were prepared. The full XPS spectrum of Fe@Cu(HBTC)-1 (Fig. S2a) highlights the existence of Fe, Cu, Cl, O, and C elements. XPS core-level spectra of the Fe@Cu(HBTC)-1 in Cu 2p, Fe 2p, and O 1s regions were plotted. As shown in Fig. S2b, the peak at 934.5 eV and the two shake-up satellites indicating the presence of divalent Cu(II). It is consistent with Cu 2p peaks of Cu(HBTC)-1. The peaks at 712.3 eV and 725.8 eV are the characteristic Fe 2p<sub>3/2</sub> and Fe 2p<sub>1/2</sub> (Fig. S2c), respectively, indicating trivalent Fe in Fe@Cu(HBTC)-1. The Cl element and trivalent Fe(III) are derived from  $\text{FeCl}_3$ . The O 1s peak (Fig. S2d) is the same as that of Cu(HBTC)-1, indicating that the Fe-BTC cannot formed through physical mixing.

### **Electron paramagnetic resonance (EPR) experiment**

In order to verify  $\bullet\text{OH}$  and  $\text{O}_2^{\bullet-}$  radicals, DMPO was used for the spin trapping agent. In a typical measurement of  $\bullet\text{OH}$ , 20  $\mu\text{L}$  of 2D Fe-BTC aqueous suspension (final concentration 100 mg/L) and 20  $\mu\text{L}$  of 500 mM  $\text{H}_2\text{O}_2$  were added into 760  $\mu\text{L}$  of 0.2 M NaAc-HAc buffer (pH 3.5). Immediately, 200  $\mu\text{L}$  of 100 mM DMPO was added into the above mixture solution and start timing. The resultant solution was extracted by quartz capillary tube and placed in a glass tube for the EPR measurement. After 5 min, the spectrum was recorded on a Bruker A300 spectrometer operated under the following conditions: 9.85 GHz of microwave frequency, 18.97 mW of microwave power, 100 kHz of modulation frequency, 1.0 G of modulation amplitude, 100 G of sweep width, 10.24 ms of time constant, 2.60 s of sweep time and  $1.0 \times 10^3$  of receiver gain. Compared with  $\bullet\text{OH}$  radicals detection, the same process was used for  $\text{O}_2^{\bullet-}$  radicals measurement except that the 2D Fe-BTC catalyst was dispersed into methanol solution. Control experiments were performed in the absence of the 2D Fe-BTC catalyst.

## Effect of temperature on the catalytic performance of the 2D Fe-BTC

In our case, the optimum temperature for the developed catalyst is 45 °C. This is because the catalytic TMB oxidation by peroxidase generates two colored products, i.e., a blue one-electron oxidation product (i.e., cation free-radical, TMB<sup>•+</sup>, its maximal absorption wavelength at 370 and 652 nm, Scheme S1) which exists in rapid equilibrium with the charge-transfer complex of TMB and its two-electron oxidation product,<sup>25f</sup> and a yellow complex of its two-electron oxidation product, which is stable at acidic conditions and has the maximal absorption wavelength at 450 nm (Scheme S1).<sup>25f</sup> When temperature is increased from 20 °C to 45 °C, the content of TMB<sup>•+</sup> grows to a maximum, leading to maximal  $A_{652}$  (Fig. S5c). While when temperature is above 45 °C, the peak at 652 nm decays due to formation of a yellow complex of two-electron oxidation product of TMB (inset in Fig. S5c) with a peak at 450 nm (Fig. S5c).



**Scheme S1.** Structure of TMB and its oxidation products.

## Glucose determination in biological samples

Glucose detection in real serum samples involves two-stage procedure. First, the glucose standard curve was constructed as follows. 0.1 mL of glucose with a varied concentration and 0.1 mL of 1 mg/mL glucose oxidase were added into 0.5 mL of 0.2 M NaAc-HAc buffer (pH 7.0) and incubated in at 37 °C for 30 min. Next, the mixture was added into 3.55 mL of 0.2 M NaAc-HAc buffer (pH 3.5) in the presence of 0.25 mL of 2 mM TMB and 0.5 mL of 100 mg/L 2D Fe-BTC. The absorbance at 652 nm was monitored after the mixture was incubated at 45 °C for 15 min. Second, the determination of glucose content in the actual sample was carried out as follows. Serum samples were filtered by ultra filtration at 3000 rpm with 30 kDa Amicon cells for 30 min, and then 100 µL of 10-fold diluted filtrate was used in place of the glucose standard in the same procedure as the glucose standard.

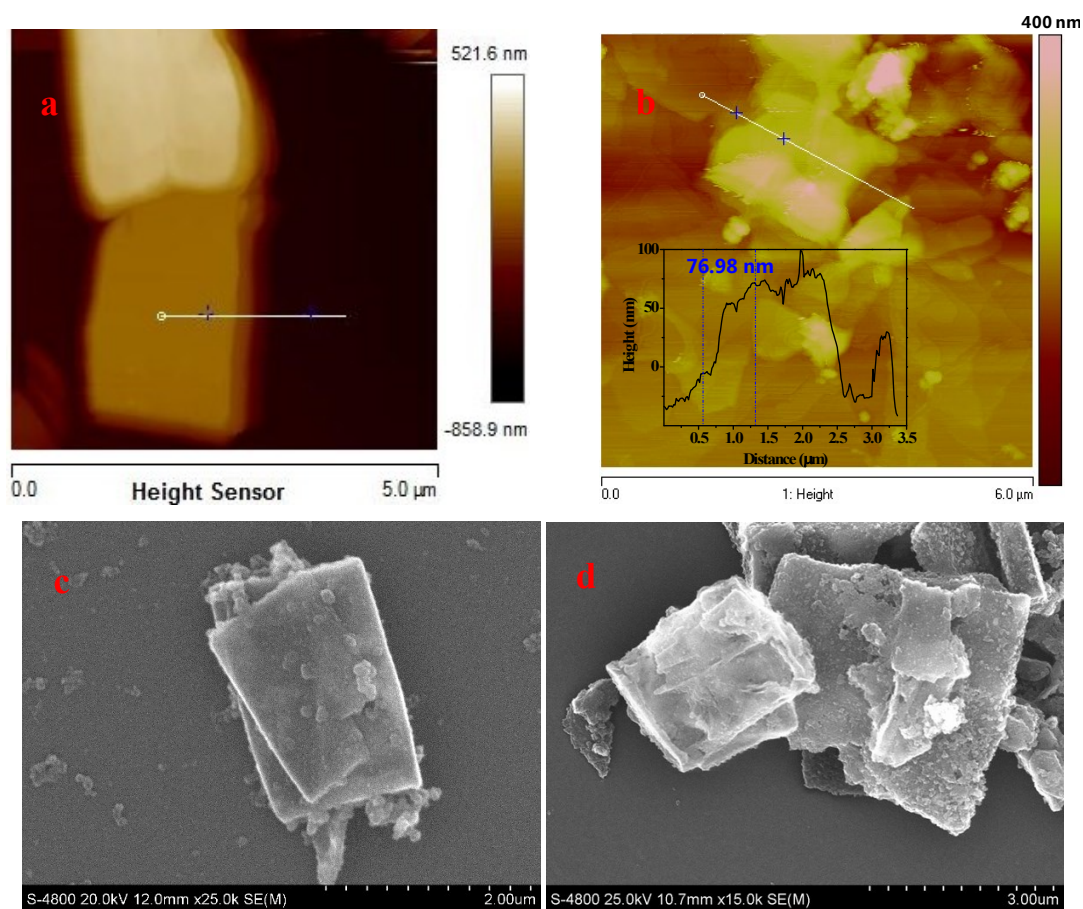


**Fig. S1.** (a) AFM image of Cu(HBTC)-1. (b) AFM image of 2D Fe-BTC. Inset shows the height mode profile with color-coded blue along the corresponding track shown in the AFM image. (c) (d) SEM images of 2D Fe-BTC.

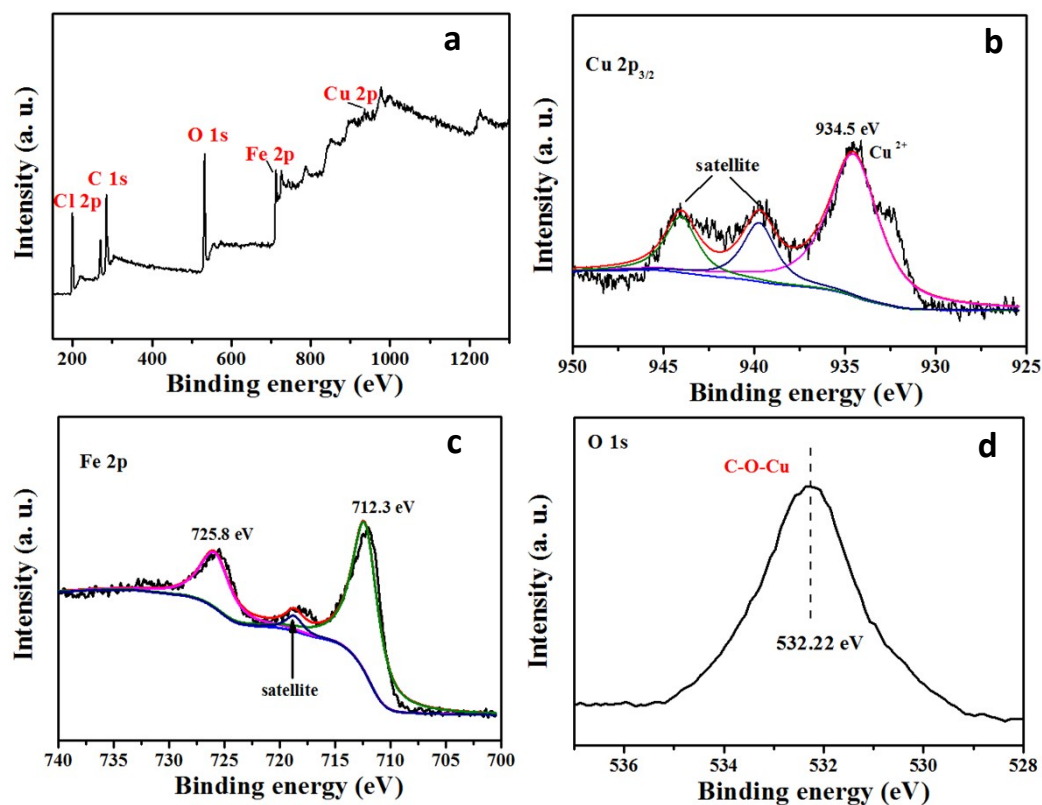


**Fig. S2.** (a) XPS survey spectrum of the Fe@Cu(HBTC)-1. (b) XPS Cu 2p peaks of the Fe@Cu(HBTC)-1. (c) XPS Fe 2p peaks of the Fe@Cu(HBTC)-1. (d) XPS O 1s peaks of Fe@Cu(HBTC)-1.

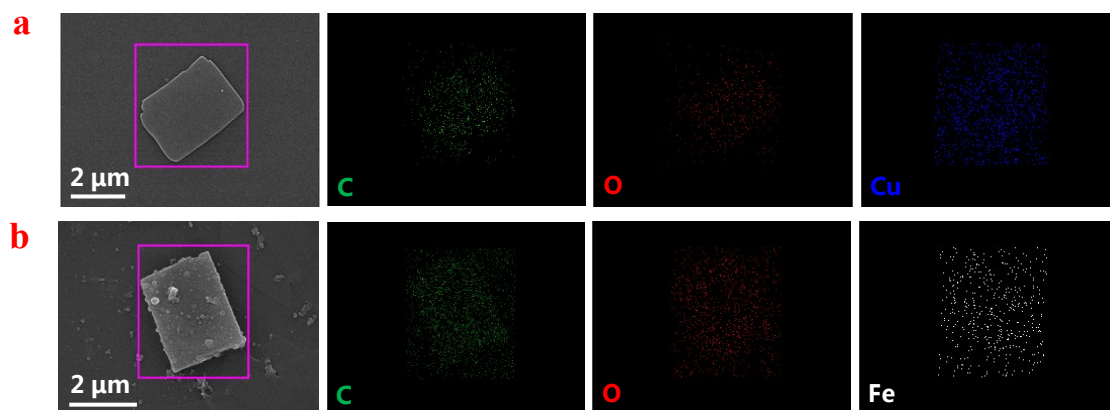


**Fig. S3.** (a) SEM-EDS (Energy dispersive spectroscopy) of the Cu(HBTC)-1; (b) SEM-EDS of the 2D Fe-BTC.

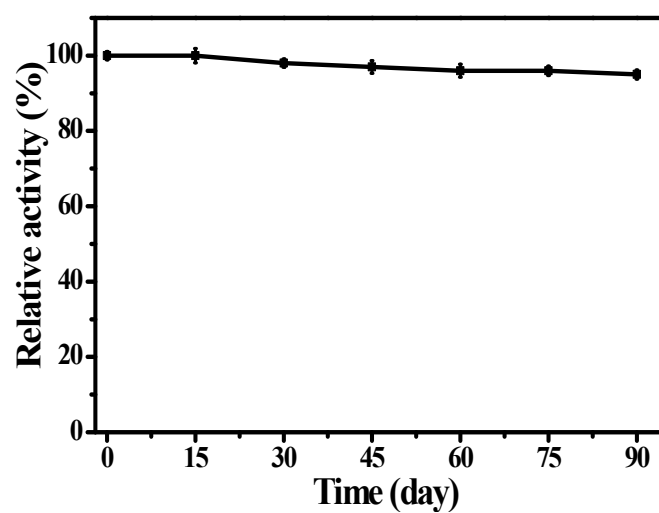


**Fig. S4.** The catalytic activity variance dependence on storage time for the 2D Fe-BTC as peroxidase mimic nanozyme. Conditions: 0.1 mM  $\text{H}_2\text{O}_2$ , 0.1 mM TMB, and 10 mg/L 2D Fe-BTC, 0.2 M acetate buffer (pH 3.5), 45 °C and 15 min. The 2D Fe-BTC solid was stored under ambient conditions for different times and used in the catalytic reaction, respectively.

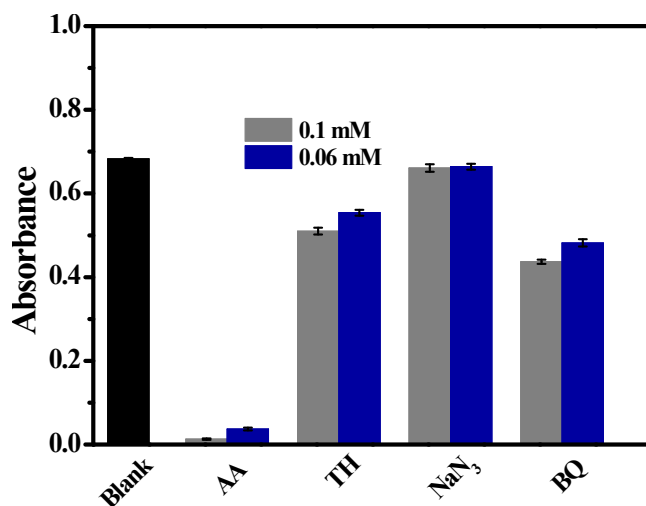


**Fig. S5.**  $A_{652}$  variance of the 2D Fe-BTC/ $H_2O_2$ /TMB system in the presence of AA, TH, BQ, and  $NaN_3$ . Reaction conditions: 0.2 M acetate buffer (pH 3.5), 0.1 mM  $H_2O_2$ , 0.1 mM TMB, 10 mg/L 2D Fe-BTC, 45 °C for 10 min reaction.

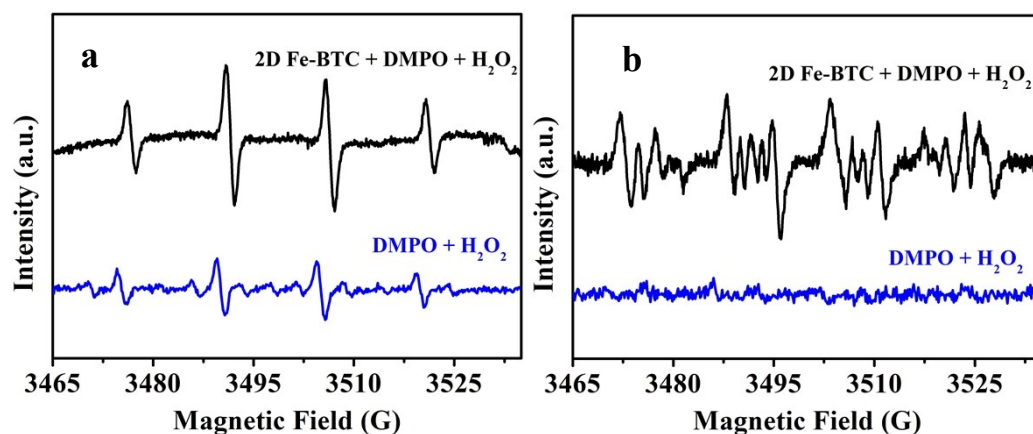


**Fig. S6.** (a) The EPR spectra of the DMPO/ $H_2O_2$  aqueous solution in the absence and presence of 2D Fe-BTC. (b) The EPR spectra of the DMPO/ $H_2O_2$  methanol solution in the absence and presence of 2D Fe-BTC. Conditions: 20 mM DMPO, 100 mg/L 2D Fe-BTC, 10 mM  $H_2O_2$ .



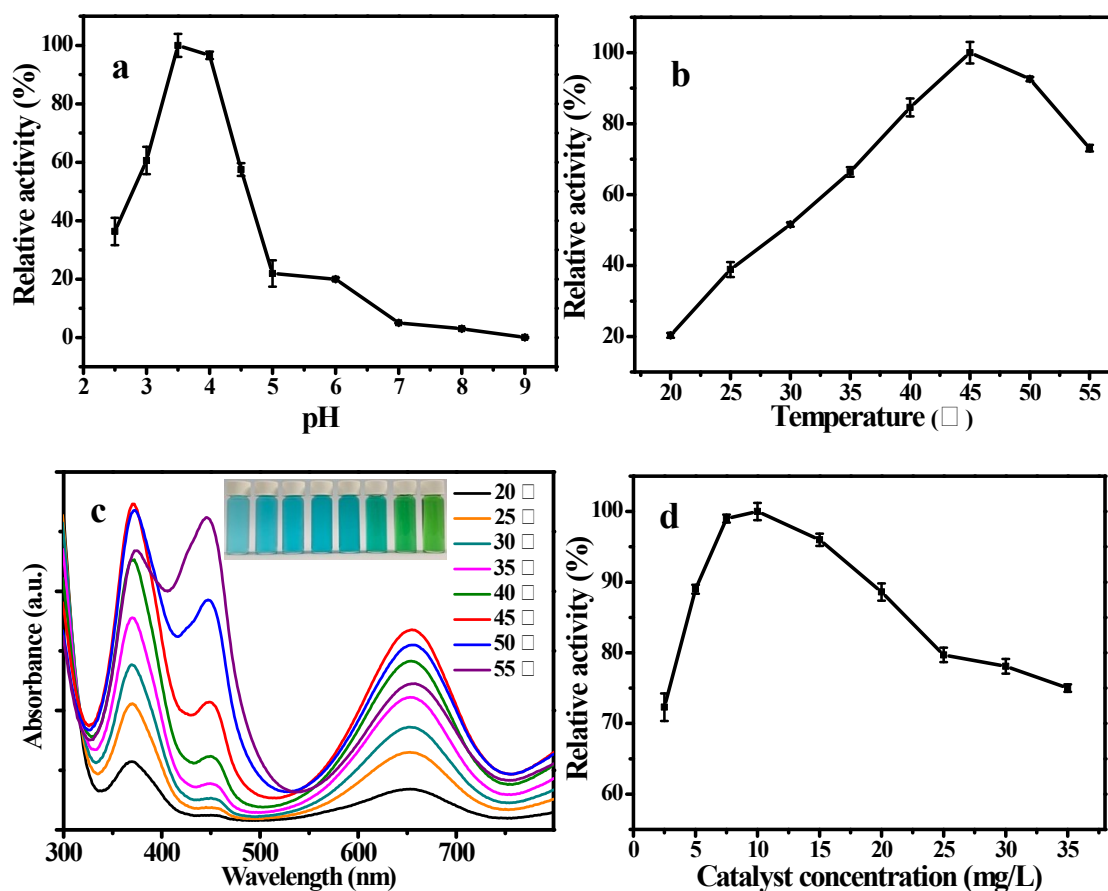


**Fig. S7.** (a) The effect of pH on the catalytic activity of 2D Fe-BTC. Reaction conditions: 10 mg/L 2D Fe-BTC, 0.1 mM H<sub>2</sub>O<sub>2</sub>, 0.1 mM TMB and 35 °C for 15 min reaction. (b) The effect of temperature on the catalytic activity of 2D Fe-BTC and (c) corresponding UV-vis spectra of the TMB/2D Fe-BTC/H<sub>2</sub>O<sub>2</sub> system at different temperatures, inset shows the image of reaction solution with varied temperatures from 20 °C to 55 °C (from left to right). Reaction conditions: 10 mg/L 2D Fe-BTC, 0.1 mM H<sub>2</sub>O<sub>2</sub>, 0.1 mM TMB and pH 3.5 (0.2 M acetate buffer) for 15 min reaction. (d) The effect of catalyst concentration on the catalytic activity of 2D Fe-BTC. Reaction conditions: 0.1 mM H<sub>2</sub>O<sub>2</sub>, 0.1 mM TMB, pH 3.5 (0.2 M acetate buffer) and 35 °C for 15 min reaction. Error bars denote standard deviations based on two measurements.

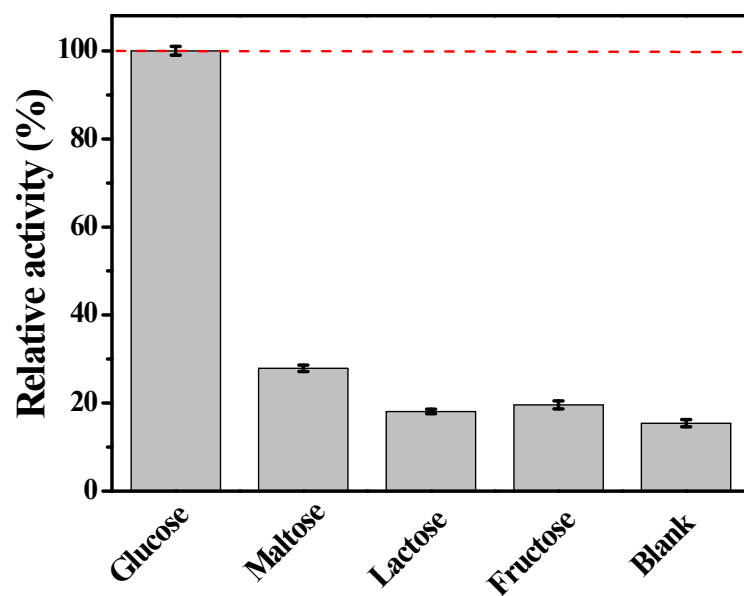


**Fig. S8.** The selectivity of glucose determination with 0.5 mM lactose, 0.5 mM fructose, 0.5 mM maltose, and 0.05 mM glucose. The error bars show the standard deviation of three measurements.

**Table S1.** Atomic concentration of the elements in 2D Cu(HBTC)-1 and 2D Fe-BTC.

| Materials     | Elements (%) |       |      |      |       |
|---------------|--------------|-------|------|------|-------|
|               | C            | O     | Cu   | Fe   | Total |
| 2D Cu(HBTC)-1 | 48.31        | 48.21 | 3.47 | /    | 100   |
| 2D Fe-BTC     | 41.94        | 54.93 | /    | 3.13 | 100   |

**Table S2.** Reproducibility between different batches of 2D Fe-BTC using the same preparation method.

| Batch No.              | 1                    | 2                     | 3                     | 4                     | SD between 4 batches |
|------------------------|----------------------|-----------------------|-----------------------|-----------------------|----------------------|
| Catalytic activity (%) | 100±1.8 <sup>a</sup> | 98.5±1.1 <sup>a</sup> | 96.1±1.5 <sup>a</sup> | 96.8±0.9 <sup>a</sup> | 1.8                  |

<sup>a</sup> Standard deviation (SD) for three duplicate determinations.

**Table S3.** Performance comparison between the 2D Fe-BTC nanozyme and other Fe-based nanozymes for the determination of H<sub>2</sub>O<sub>2</sub> and glucose in terms of linear range and LOD.

| Catalyst   | H <sub>2</sub> O <sub>2</sub> |       | Glucose      |       | Ref       |
|--|-------------------------------|-------|--------------|-------|-----------|
|  | Linear range                  | LOD   | Linear range | LOD   |           |
|  | (μM)                          | (μM)  | (μM)         | (μM)  |           |
| MIL-53(Fe) by CE                                 | 0.95 – 19                     | 0.13  | /            | /     | [4]       |
| Fe-MIL-88NH <sub>2</sub>                         | 0.2 – 200                     | /     | 2 – 300      | 0.48  | [5]       |
| MIL-68(Fe)                                       | 3 – 40                        | 0.256 | /            | /     | [6]       |
| MIL-100(Fe)                                      | 3 – 40                        | 0.155 | /            | /     | [7]       |
| Glycine-MIL-53(Fe)                               | 0.10 – 10                     | 0.049 | 0.25 – 10    | 0.13  | [23]      |
| MIL-53(Fe) by MW                                 | 0.25 – 20                     | /     | 0.25 – 20    | 0.25  | [24a]     |
| Fe <sub>3</sub> O <sub>4</sub> @MS NPs           | 1 – 100                       | 1     | 10 – 500     | 4     | [26]      |
| Fe <sub>3</sub> O <sub>4</sub> @C nanostructures | 1 – 20                        | 0.39  | 1 – 10       | 1.12  | [27]      |
| Fe <sub>3</sub> S <sub>4</sub> MNPs              | 1 – 50                        | 0.13  | 2 – 100      | 0.16  | [28]      |
| Fe-g-C <sub>3</sub> N <sub>4</sub>               | 0.5 – 50                      | 0.05  | 0.5 – 50     | 0.5   | [29]      |
| HRP  | /                             | /     | 400 – 15000  | 400   | [24c]     |
| 2D Fe-BTC  | 0.04 – 30                     | 0.036 | 0.04 – 20    | 0.039 | This work |